Magnetoelastic coupling in hexagonal multiferroic $YMnO_3$ using ultrasound measurements

Mario Poirier and Francis Laliberté
Regroupement Québécois sur les Matériaux de Pointe, Département de Physique, Université de Sherbrooke, Sherbrooke, Québec, Canada J1K 2R1

Loreynne Pinsard-Gaudart and Alexandre Revcolevschi
ICMMO, Université Paris-Sud, UMR8182-CNRS, 91405 Orsay, France
(Received 3 August 2007; revised manuscript received 14 September 2007; published 15 November 2007)

We report an ultrasonic investigation of the elastic moduli on a single crystal of hexagonal $YMnO_3$ as a function of temperature. Stiffening anomalies in the antiferromagnetic Néel state below $T_N=72.4$ K are observed on all the four elastic moduli C_{ii}. The anomalies are the most important on C_{11} and C_{66} for in-plane elastic deformations; this is consistent with a strong coupling of the lattice with the in-plane exchange interactions. We use a Landau free energy model to account for these elastic anomalies. We derive an expression which relates the temperature profile of the anomaly to the order parameter; the critical exponent associated with this parameter $\beta=0.42$ is not consistent with a chiral *XY* or three-dimensional Heisenberg universality class, but more in agreement with a conventional antiferromagnetic long-range order. A tiny softening anomaly on C_{11} for which hysteresis effects are observed could be indicative of an interaction between ferroelectric and magnetic domains at T_N. Moreover, magnetic fluctuation effects both above and below T_N are identified through abnormal temperature and magnetic field effects.

DOI: 10.1103/PhysRevB.76.174426 PACS number(s): 75.47.Np, 75.50.Ee, 75.40.Cx

I. INTRODUCTION

Hexagonal $YMnO_3$ is one of the best known examples of multiferroics, a material that possesses both ferroelectricity and magnetism. The ferroelectric (FE) transition occurs at a relatively high temperature above 900 K. Below the Curie temperature, the compound crystallizes in a hexagonal structure with the space group $P6_3cm$.[1] The Mn^{3+} ($S=2$) ions form nearly triangular networks in $z=0$ and $z=1/2$ layers which stack in the *ABAB* sequence along the z axis with a wide separation introduced by the intervening Y and O ions.[2] This suggests a predominant two-dimensional (2D) character in the *ab* plane. For this system, the geometrical frustration of the antiferromagnetic (AF) spins on the triangular lattice results in the 120° spin ordering below the Néel temperature $T_N \sim 70$ K.

The Curie-Weiss temperature deduced from susceptibility measurements is approximately ten times higher than T_N (Refs. 2–4) and the magnetic moment is lower than the expected value from the fully polarized Mn^{3+}.[2,3,5] This reduction in T_N and magnetic moment is consistent with strong spin fluctuations due to geometrical frustration and/or low dimensionality. The coexistence of novel magnetism and ferroelectricity suggests a peculiar interaction between the spins and the lattice degrees of freedom, although the low T_N, compared to the ferroelectric transition, infers weak coupling between magnetism and ferroelectricity. Although various crystallographic, optical, and magnetic structural studies have been performed to characterize independently the FE and magnetic properties,[1,3,6] only a few ones have been directed to understand their interrelation. Dielectric constant,[4] specific heat,[7,8] and thermal conductivity[9,10] experiments revealed a spin-lattice coupling whose understanding remains an open question. As far as magnetism is concerned, neutron scattering studies[11–14] have reported the presence of unconventional spin fluctuations both above and below T_N that could be related to the anomalous increase of the thermal conductivity upon magnetic ordering.[9] However, the question of coexistence of long-range order with significant spin fluctuations in the Néel state for the triangular lattice remains. The symmetry of the order parameter and the nature of the universality class associated with the 120° spin structure are also not resolved up to now.

To investigate the coupling between magnetism and the lattice degrees of freedom in $YMnO_3$, we report an ultrasonic investigation of the elastic moduli of a single crystal in the temperature range 2–150 K, both above and below the spin ordering temperature T_N. Although elastic anomalies at T_N are observed on all studied moduli, an important coupling of the magnetic order parameter is only obtained with an in-plane strain field. A Landau free energy expansion is used to interpret these anomalies and a critical analysis of the temperature behavior just below T_N is tentatively given. Small temperature hysteretic effects are observed, indicating a domain structure. A peculiar temperature profile above T_N for two moduli is discussed in relation with the magnetic fluctuation issue.

II. EXPERIMENT

High quality $YMnO_3$ single crystals are grown using the standard floating zone technique. Powder x-ray diffraction measurements confirmed that the crystal investigated here has the $P6_3cm$ hexagonal structure at room temperature [$a=b=6.1380(1)$ Å, $c=11.4045(1)$ Å]. A single crystal was then oriented with a back Laue x-ray diffraction technique and cut with a wire saw to obtain two sets of parallel faces respectively oriented perpendicular (separation distance of 3.29 mm) and parallel (3.54 mm) to the hexagonal c axis. The faces were subsequently polished to obtain a mirrorlike

TABLE I. Elastic moduli of $YMnO_3$ (units: 10^{10} N/m^2) at 4 K.

C_{11}	C_{33}	C_{44}	C_{66}
18.5±0.1	29.8±0.5	9.86±0.15	5.94±0.05

aspect. We used a pulsed-echo ultrasonic technique in the reflection mode to measure the velocity and magnitude of longitudinal and transverse waves propagating along both directions. The plane acoustic waves were generated with $LiNbO_3$ piezoelectric transducers (fundamental frequency of 30 MHz and odd overtones) bonded to one parallel face with silicon seal. The technique consists in measuring the phase shift and the amplitude of the first elastic pulse reflected from the opposite parallel face. Doing so, this technique yields only velocity and attenuation variations; an absolute value of the velocity is obtained by measuring the transit time between different reflected echoes. The crystal was mounted in a variable temperature insert; the useful temperature range was 2–150 K, the maximum value being imposed by phase transformation of the silicon seal around 200 K. A magnetic field up to 14 T could be applied along different directions.

For a crystal having hexagonal symmetry, the elastic modulus matrix has only five nonzero independent components C_{ij}.[15] Four of these components can be obtained by propagating ultrasonic waves parallel and perpendicular to the hexagonal c axis and by measuring the velocity of these waves with various polarizations (longitudinal and transverse). For propagation along c, the longitudinal and transverse velocities are, respectively, given by $V_{L1}=(C_{33}/\rho)^{1/2}$ and $V_{T1}=(C_{44}/\rho)^{1/2}$. For the perpendicular direction, besides the longitudinal one, two transverse velocities (polarization $\perp c$ and $\|c$) are obtained: $V_{L2}=(C_{11}/\rho)^{1/2}$, $V_{T\perp}=(C_{66}/\rho)^{1/2}$, and $V_{T\|}=(C_{44}/\rho)^{1/2}$. By using the density $\rho=5.1$ g/cm^3 and the experimental velocities, the four C_{ij} are obtained. We notice that V_{T1} and $V_{T\|}$ are equal if the crystal is correctly oriented, a situation that was checked in our experiment. The absolute values of the moduli at low temperatures are given in Table I.

III. RESULTS

The coupling between the lattice and the spin degrees of freedom generally yields anomalies on selected elastic moduli when three-dimensional magnetic order sets in. The selection is imposed by the nature of the coupling between the elastic deformation and the order parameter, coupling which is highly sensitive on the symmetry of the latter. This coupling is confirmed for all elastic moduli investigated in the present work on multiferroic hexagonal $YMnO_3$. Our ultrasonic velocity measurements have been performed at different frequencies between 30 and 300 MHz; no significant frequency dependence was noticed on the velocity. The data presented below were all obtained at 103 MHz. At this frequency, the noise level is so small (better than 1 ppm) that no error bars appear in the presented plots. All the temperature profiles were obtained when warming the crystal from 2 K.

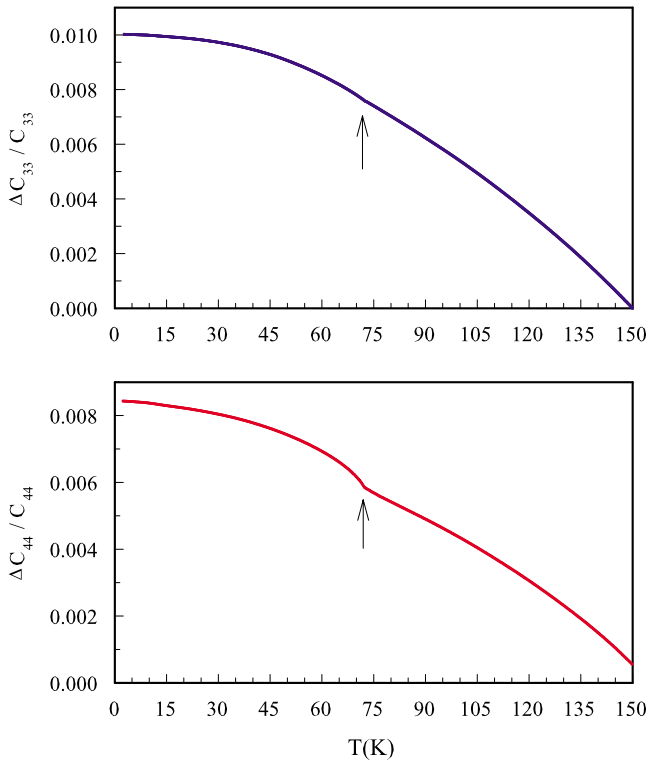

FIG. 1. (Color online) Temperature profile of $\Delta C_{33}/C_{33}$ and $\Delta C_{44}/C_{44}$. T_N is indicated by an arrow.

In Fig. 1, we present the temperature profile of the relative variation of the two elastic moduli that are the least affected by magnetic ordering, $\Delta C_{33}/C_{33}$ and $\Delta C_{44}/C_{44}$. When the temperature is decreased from 150 K, the modulus C_{33} which implies a pure compression along the c axis smoothly increases and saturates at low temperature. This temperature profile appears normal in view of the expected stiffening following the progressive disappearance of phonon anharmonic effects at low temperatures. There is, however, a small increase of slope below 72 K, indicating a further stiffening when AF ordering occurs at T_N. C_{44}, related to a shear deformation in a plane containing the c axis, presents a similar temperature profile. There is, however, a much more pronounced upturn of the modulus below 72.5 K, confirming a definite stiffening below T_N ($\sim$0.1%).

The temperature profile of the relative variation of the other two moduli appears both similar and different from the previous ones and, in a sense, less normal. These data are presented in Fig. 2 over the same temperature range. C_{11}, corresponding to a pure compression in the ab plane, increases weakly below 150 K and, on this scale, appears to saturate around 90 K. Then, an abrupt stiffening begins at $T_N=72.4$ K until saturation is obtained below 15 K; the amplitude of the stiffening is approximately 1%. C_{66} is also associated with in-plane deformations and it shows a nonconventional behavior. The modulus decreases below 150 K until a minimum is reached around 75 K; then, it increases further ($\sim$3%) with a clear increase in slope near 72 K. Below 72 K, the thermal profile resembles the one observed on C_{11}.

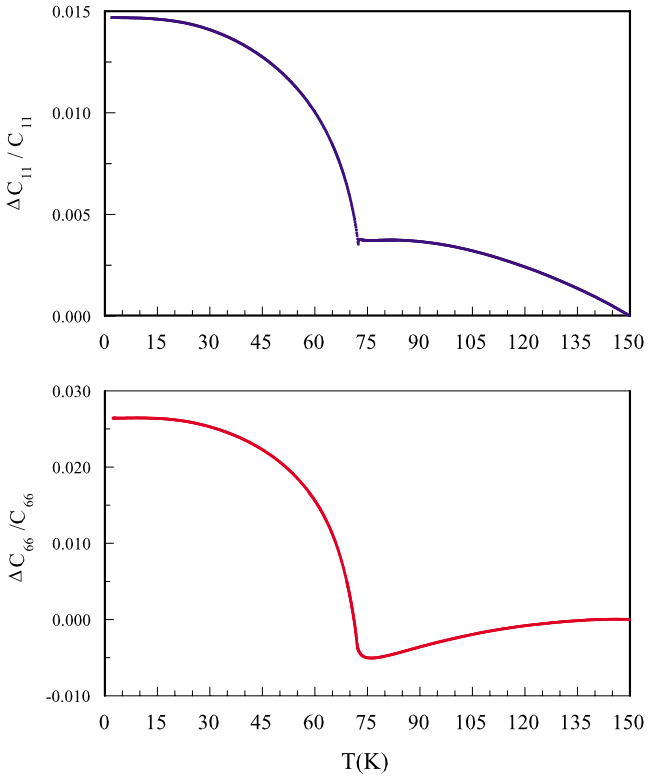

FIG. 2. (Color online) Temperature profile of $\Delta C_{11}/C_{11}$ and $\Delta C_{66}/C_{66}$.

It appears then that the four elastic moduli investigated here, C_{11}, C_{33}, C_{44}, and C_{66}, stiffen progressively below the Néel temperature T_N=72.4 K. Moreover, the temperature profile of the anomalies seems to mimic the AF magnetic order parameter, the magnetic moment $\mathbf{m}(T)$.[3,11] It is worth to notice that significant elastic anomalies are observed for moduli implying elastic deformation (compression and shear) only in the *ab* plane, C_{11} and C_{66}; these are also the only moduli to present an unconventional elastic behavior above T_N. These observations appear consistent with a two-dimensional character of the magnetic properties. Moreover, since the anomaly on C_{33} is very small, this means that interplane exchange interactions J_1' and J_2' are not strongly coupled to the lattice compared to in-plane ones, J_1 and J_2, which yield an important anomaly on C_{11} in agreement with the analysis of spin fluctuations.[12] The analysis of the temperature dependence of these anomalies is highly delicate since it necessitates a precise knowledge of the overall temperature background both above and below T_N. Such an analysis appears difficult for C_{33} because the amplitude of the anomaly is too small compared to the total modulus variation with temperature. However, this could be done for C_{11} and C_{66} since the amplitudes of the anomalies, respectively, around 1% and 3%, are much larger. It will also be attempted for C_{44} even if the variation is only around 0.1%.

Before doing so, let us examine more precisely the temperature profile of C_{11} just above T_N. The relative variation $\Delta C_{11}/C_{11}$ (relative to the value at 100 K) is presented in Fig. 3. The modulus C_{11} increases smoothly as the temperature is decreased from 100 K; then, it goes through a maximum around 82 K, reaches a minimum just above 75 K, and increases further before reaching the AF transition. A sharp downward step (0.02%) occurs below 72.8 K before an abrupt upturn at 72.4 K, signaling a progressive stiffening. This abrupt downward step preceding a stiffening is accompanied by a small hysteresis (0.4 K) when sweeping the temperature up and down through the transition, as shown in the inset of Fig. 3. The temperature profile above T_N is only modified up to 75 K where a local minimum is observed. We said previously that the thermal profile of the moduli is not frequency dependent. For C_{11}, however, a small upward shift as a function of frequency is observed for $T_N < T < 90$ K; an example of this is presented in Fig. 3 for two frequencies. This shift is 200 times smaller than the stiffening below T_N and, if it is significant, it could be related to a domain structure generally expected when hysteresis is observed. Although they show hysteresis, the other moduli do not show any frequency effects or a downward step at T_N. A minimum is, however, observed on C_{66} near 75 K (Fig. 2), minimum that could be a signature of C_{11} since $C_{66}=\frac{1}{2}(C_{11}-C_{12})$.

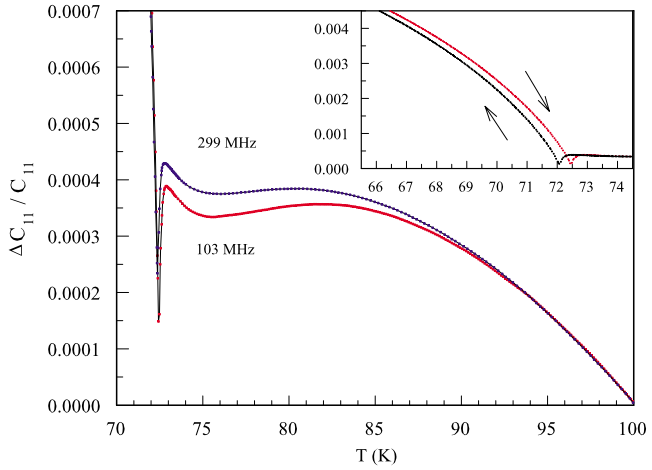

FIG. 3. (Color online) Temperature profile of the relative variation of the elastic modulus C_{11} at two frequencies, 103 and 299 MHz, on reduced scales for $T > T_N$. Inset: Hysteresis near T_N at 103 MHz, arrows indicating the direction of the temperature sweeps.

IV. DISCUSSION

In ferroelectric $YMnO_3$, there is a possibility to find piezoelectricity since a remnant polarization is observed.[16] It is known that a piezoelectric character can stiffen specific elastic moduli determined by symmetry.[15] In strong piezoelectric materials, this stiffening can reach a few percents. In $YMnO_3$, these effects should be small and they would be included in the absolute values of the moduli given in Table I. Thus, possible piezoelectric effects will not be discussed further. The effects of magnetic frustration in the stacked triangular lattice have been the object of many studies over the years[17] and ultrasonic techniques[18–20] have been used extensively as a means to obtain the magnetic phase diagram of ABX_3 systems. Similar to what has been done in these systems, we can use a phenomenological Landau model to ac-

TABLE II. Relative values of the coupling constant $g_{i,2}$.

$g_{1,2}$	$g_{3,2}$	$g_{4,2}$	$g_{6,2}$
1.0	0.04(1)	0.05(1)	0.90(5)

count for the observed changes in the elastic properties of $YMnO_3$. If one takes into account the coupling between the order parameter Q and the strain e_i, three terms contribute to the free energy $F(Q,e_i)$.

$$F(Q,e_i) = L(Q) + F_{el}(e_i) + F_c(Q,e_i), \tag{1}$$

where $L(Q)$ is the Landau-type free energy expressed in terms of a power series of the order parameter Q, $F_{el}(e_i)$ the elastic energy associated with the deformations, and $F_c(Q,e_i)$ the coupling between the strain e_i and the order parameter Q. Because of the 120° spin arrangement in the *ab* plane[3,12] in the absence of a magnetic field, we can write with in-plane spin component $S_\perp$ as the order parameter (we neglect any S_z component),

$$L(S_\perp) = aS_\perp^2 + bS_\perp^4. \tag{2}$$

The elastic energy for a hexagonal structure is given by[15]

$$F_{el}(e_i) = \tfrac{1}{2}C_{11}(e_1^2 + e_2^2) + \tfrac{1}{2}C_{33}e_3^2 + \tfrac{1}{2}C_{44}(e_4^2 + e_5^2) + \tfrac{1}{2}C_{66}e_6^2 + C_{12}e_1e_2 + C_{13}(e_1e_3 + e_2e_3), \tag{3}$$

where C_{ij} represent the bare elastic moduli in the high-temperature phase. For the coupling term, time inversion symmetry imposes a quadratic dependence on the order parameter, $S_\perp^2$: the coupling term associated with the strain e_i can thus be written as

$$F_c(S_\perp,e_i) = g_{i,r}S_\perp^2 e_i^r, \tag{4}$$

where $g_{i,r}$ is the coupling constant associated with the deformation e_i elevated to the power r. The term with $r=2$ is always allowed whatever the symmetry but $r=1$ implies inequivalence of $|e_i|$ and $-|e_i|$. If we minimize the Landau energy relative to the strain e_i, we obtain a spontaneous strain $e_i(S_\perp)$ which is used to derive the elastic constant C'_{ij}.[21] The biquadratic coupling term ($r=2$) leads to a stiffening of the elastic constant C_{ii} according to the general form

$$C'_{ii} = C_{ii} + 2g_{i,2}S_\perp^2. \tag{5}$$

For the case of linear-quadratic coupling ($r=1$), a negative step is obtained according to

$$C'_{ii} = C_{ii} - \frac{g_{i,1}^2}{2b}. \tag{6}$$

The results presented in Figs. 1 and 2 are consistent with the prediction of Eq. (5), a stiffening related to $S_\perp$.[2] We give in Table II the relative value of the coupling constant $g_{i,2}$ as deduced from Figs. 1 and 2. The largest constant is obtained for C_{11} and $g_{1,2}$ is thus taken as 1; $g_{6,2}$ associated with C_{66} is also very important around 0.9. The constants $g_{3,2}$ and $g_{4,2}$ are found smaller by a factor between 20 and 25. This anisotropy of the coupling to the order parameter appears consistent with the one observed in the in-plane and interplane exchange constants[12] and with an *XY* symmetry.

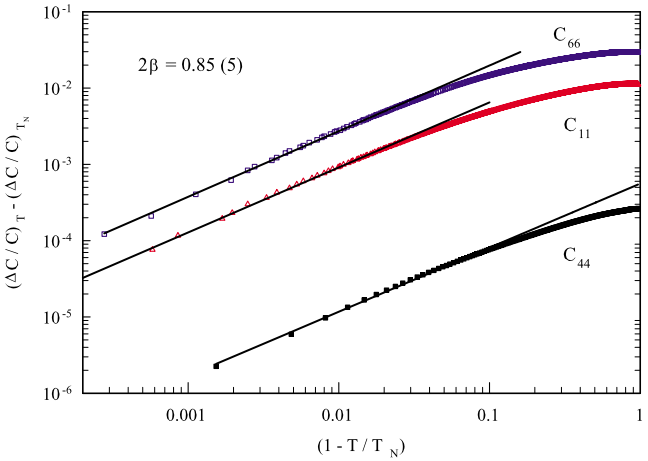

FIG. 4. (Color online) Relative variation of the elastic moduli C_{11}, C_{44}, and C_{66} as a function of the reduced temperature $(1-T/T_N)$. Straight lines represent fits to Eq. (7).

We have then tried to analyze the variation of the elastic moduli C_{11}, C_{44}, and C_{66} relative to their value at T_N by fitting the order parameter to $S_\perp \sim (1-T/T_N)^\beta$ near the critical temperature T_N.

$$\frac{\Delta C_{ii}}{C_{ii}} = D_i(1 - T/T_N)^{2\beta}, \tag{7}$$

where D_i is a constant depending on $g_{i,2}/C_{ii}$. This analysis for C_{11} and C_{66} is surely more valid than for C_{44} since the anomalies are at least ten times larger at T_N. The results of this analysis are presented in Fig. 4 on a log-log scale. Not only the overall temperature dependence appears very similar for C_{11} and C_{66}, but the same exponent $2\beta=0.85(5)$ is obtained with $T_N=72.43(5)$. Surprisingly, the same exponent is also found for C_{44}, which means that the overall temperature profile of the background near T_N is not important to determine the critical behavior. Also, hysteresis effects were found to only affect T_N (Fig. 3), not the exponent. The value $\beta=0.42(3)$, which is obtained over only two decades of the reduced temperature, is neither consistent with chiral *XY* (0.25) and chiral Heisenberg (0.30) universality classes or with *XY* (0.35) and Heisenberg (0.36) ones.[17] Although this appears to contradict our previous observation pertaining to the coupling constants, it is clear in Fig. 4 that the same physical phenomenon is at the origin of the elastic anomalies on C_{11} and C_{66}, and by extension on the other two moduli. The AF order parameter $S_\perp$ has been associated with three-dimensional (3D) Heisenberg or 3D *XY* symmetry classes from specific heat[7] and muon-spin relaxation[22] studies; our study is, however, not able to resolve this issue.

Finally, the sharp downward step observed on C_{11} [Fig. 3(a)] could be consistent with the prediction of Eq. (6). On the one hand, the observation of hysteresis in the vicinity of this peak could be consistent with weak ferromagnetism, although this has been observed only in $ScMnO_3$.[3] On the other hand, coupling between magnetic and electric domains

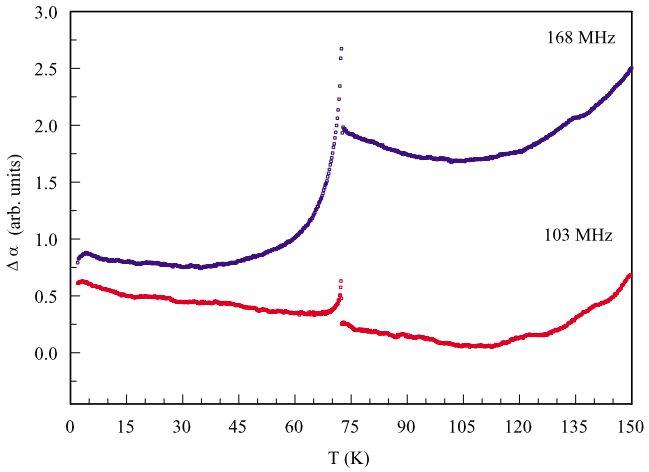

FIG. 5. (Color online) Variation of the attenuation $\Delta\alpha$ of in-plane compression waves as a function of temperature at two frequencies, 103 and 168 MHz.

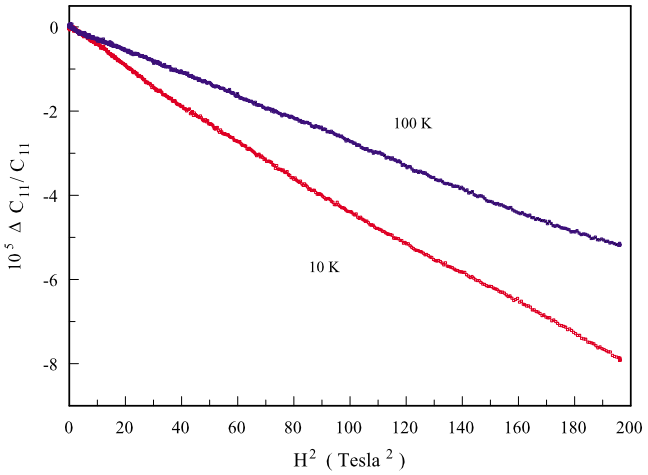

FIG. 6. (Color online) Relative variation of C_{11} as a function of the magnetic field at two temperatures well below and above T_N.

in $YMnO_3$ has been reported by imaging with optical second harmonic generation;[23] it has been suggested that the small anomaly observed on the in-plane dielectric constant[24] could result from such coupling effects on domain walls.[25] The small peak on C_{11} at T_N together with the observation of hysteresis could result from an interaction between in-plane compression waves and the domain walls.

Previous neutron scattering studies[12–14] reported the presence of unconventional spin fluctuations both above and below T_N. These fluctuations could explain the anomalous behavior of C_{11} (and by extension C_{66}) well above T_N, as shown in Fig. 3(a). Since similar effects are not observed for C_{33} and C_{44}, fluctuations preferentially 2D-like associated with in-plane exchange constants are likely responsible. The ultrasonic attenuation is generally more sensitive to fluctuations since it is a dissipative phenomenon. These attenuation variations $\Delta\alpha$ are difficult to obtain with precision on a wide temperature range and this is why they must be interpreted with great care. We present in Fig. 5 the variation of the attenuation associated with the C_{11} modulus as a function of temperature at two frequencies. As the temperature is decreased from high temperature, the attenuation generally decreases because the scattering of the acoustic waves by phonons is reduced. Here, the attenuation shows a minimum at a rather high temperature near 110 K for both frequencies and it increases for lower temperatures, a behavior that is not consistent with decreasing phonon scattering. At 103 MHz, the AF ordering produces a very sharp peak at T_N but does not change significantly the monotonous increase of the attenuation that begun near 110 K and the attenuation increases down to the lowest temperature. At 168 MHz, the temperature profile from 150 to 72 K is conserved; however, the peak is more pronounced at T_N and the attenuation decreases rapidly below the Néel temperature. At lower temperature, there is no saturation of the attenuation but a small increase below 30 K is observed. These attenuation data strongly suggest that spin degrees of freedom, in other words, magnetic fluctuations both above (at least up to 110 K) and below T_N, dissipate acoustic energy. At T_N, the sharp increase is due to the spontaneous strain yielding to Eq. (6) and for which hysteresis is observed. Below T_N, spin degrees of freedom are lost when 3D AF ordering occurs and the attenuation decreases rapidly. The data reveal an increase of attenuation at temperatures much higher than T_N and a reduction below when 3D AF ordering occurs. Although this reduction increases rapidly in amplitude with frequency, dissipation still occurs well below T_N. These observations are consistent with *extraordinary spin-phonon interactions* deduced from thermal conductivity data.[9] How these fluctuations are related to the domain structure remains an open question. The presence of domains and fluctuations near T_N could complicate the analysis of the critical behavior presented in Fig. 4 and affect the determination of the exponent β.

The magnetic character of the peculiar behavior of C_{11} above T_N can also be revealed by a magnetic field analysis. Up to 14 T, we did not find any measurable variation of T_N whatever the orientation of the field relative to the c axis was. This probably implies that the amplitude of the magnetic order parameter below T_N is highly rigid relative to the magnetic field. Nevertheless, some magnetic field effects can be measured on C_{11} over the 2–150 K temperature range. These are presented in Fig. 6 as C_{11} variations relative to the value at zero field. The data are presented as a function of H^2 at two temperatures, 10 K, well below T_N, and 100 K, well above for a field applied parallel to the c axis. The field profile is very similar for both temperatures and the absolute value has not even decreased by a factor 2 when the temperature has been multiplied by 10. These effects have thus to be related to the overall background: a magnetic field enhances the softening of C_{11} both above and below T_N, confirming the existence of important magnetic fluctuations in this geometrically frustrated magnet, fluctuations that are likely enhanced by a magnetic field. It has been suggested from heat capacity data[7] that a single Einstein contribution could adequately fit the low-temperature deviation, indicating that there is no evidence of an anomalous magnetic contribution for $T < T_N$. Our data do not support this suggestion.

V. CONCLUSION

In conclusion, our ultrasonic experiments have identified an important coupling between the AF order parameter and the lattice in hexagonal $YMnO_3$. This coupling yields important stiffening anomalies below T_N only for in-plane elastic deformations, compression and shear. This implies that the coupling is established via the modulation of the in-plane exchange interactions. The critical exponent β for the AF order parameter near T_N is found higher than the expected value from *XY* and 3D Heisenberg universality classes. This situation favors a conventional antiferromagnetic long-range ordering as suggested from other measurements. However, the data confirm important spin fluctuations over a wide temperature range above and below the Néel temperature. Finally, a sharp step appearing on C_{11} at T_N, for which hysteresis is observed, is consistent with a weak coupling between ferroelectricity and magnetism at domain walls.

ACKNOWLEDGMENTS

The authors thank G. Quirion, S. Jandl, and C. Bourbonnais for discussions and M. Castonguay for technical support. This work was supported by grants from the Fonds Québécois de la Recherche sur la Nature et les Technologies (FQRNT) and from the Natural Science and Engineering Research Council of Canada (NSERC).

[1] H. L. Yakel, W. C. Koehler, E. F. Bertaut, and E. F. Forrat, Acta Crystallogr. **16**, 957 (1963).
[2] T. Katsufuji, M. Masaki, A. Machida, M. Moritomo, K. Kato, E. Nishibori, M. Takata, M. Sakata, K. Ohoyama, K. Kitazawa, and H. Takagi, Phys. Rev. B **66**, 134434 (2002).
[3] A. Muñoz, J. A. Alonso, M. J. Martínez-Lope, M. T. Casáis, J. L. Martínez, and M. T. Fernández-Díaz, Phys. Rev. B **62**, 9498 (2000).
[4] T. Katsufuji, S. Mori, M. Masaki, Y. Moritomo, N. Yamamoto, and H. Takagi, Phys. Rev. B **64**, 104419 (2001).
[5] M. Bieringer and J. E. Greedan, Solid State Chem. **143**, 132 (1999).
[6] M. N. Iliev, H.-G. Lee, V. N. Popov, M. V. Abrashev, A. Hamed, R. L. Meng, and C. W. Chu, Phys. Rev. B **56**, 2488 (1997).
[7] M. Tachibana, J. Yamazaki, H. Kawaji, and T. Atake, Phys. Rev. B **72**, 064434 (2005).
[8] D. G. Tomuta, S. Ramakrishnan, G. J. Nieuwenhuys, and J. D. Mydosh, J. Phys.: Condens. Matter **13**, 4543 (2001).
[9] P. A. Sharma, J. S. Ahn, N. Hur, S. Park, Sung Baek Kim, Seongsu Lee, J.-G. Park, S. Guha, and S.-W. Cheong, Phys. Rev. Lett. **93**, 177202 (2004).
[10] J.-S. Zhou, J. B. Goodenough, J. M. Gallardo-Amores, E. Morán, M. A. Alario-Franco, and R. Caudillo, Phys. Rev. B **74**, 014422 (2006).
[11] Th. Lonkai, D. Hohlwein, J. Ihringer, and W. Prandl, Appl. Phys. A: Mater. Sci. Process. **74**, S843 (2002).
[12] T. J. Sato, S. -H. Lee, T. Katsufuji, M. Masaki, S. Park, J. R. D. Copley, and H. Takagi, Phys. Rev. B **68**, 014432 (2003).
[13] J. Park, J.-G. Park, G. S. Jeon, H.-Y. Choi, C. Lee, W. Jo, R. Bewley, K. A. McEwen, and T. G. Perring, Phys. Rev. B **68**, 104426 (2003).
[14] B. Roessli, S. N. Gvasaliya, E. Pomjakushina, and K. Conder, JETP Lett. **81**, 351 (2005).
[15] E. Dieulesaint and D. Royer, *Ondes Élastiques dans les Solides* (Masson, Paris, 1974), p. 121.
[16] H. Kitahata, K. Tadanaga, T. Minami, N. Fujimura, and T. Ito, J. Sol-Gel Sci. Technol. **19**, 589 (2000).
[17] M. F. Collins and O. A. Petrenko, Can. J. Phys. **75**, 605 (1997).
[18] Y. Trudeau, M. L. Plumer, M. Poirier, and A. Caillé, Phys. Rev. B **48**, 12805 (1993).
[19] G. Quirion, T. Taylor, and M. Poirier, Phys. Rev. B **72**, 094403 (2005).
[20] G. Quirion, X. Han, M. L. Plumer, and M. Poirier, Phys. Rev. Lett. **97**, 077202 (2006).
[21] W. Rewald, Adv. Phys. **22**, 721 (1973).
[22] T. Lancaster, S. J. Blundell, D. Andreica, M. Janoschek, B. Roessli, S. N. Gvasaliya, K. Conder, E. Pomjakushina, M. L. Brooks, P. J. Baker, D. Prabhakaran, W. Hayes, and F. L. Pratt, Phys. Rev. Lett. **98**, 197203 (2007).
[23] M. Fiebig, Th. Lottermoser, D. Frölich, A. V. Gottsev, and R. V. Pisarev, Nature (London) **419**, 818 (2002).
[24] Z. J. Huang, Y. Cao, Y. Y. Sun, Y. Y. Xue, and C. W. Chu, Phys. Rev. B **56**, 2623 (1997).
[25] J. H. Qiu and Q. Jiang, Phys. Rev. B **73**, 024406 (2006).